Contents

List of Tables

List of Figures

I. Introduction

This report details the development of a semi-autonomous aerial transport vehicle designed to carry a single passenger and operate in critical and emergency environments. Developed for the GoAERO Competition, this innovative concept features advanced onboard sensors and autonomous recognition systems to navigate obstacles and adapt to adverse conditions. Key features include semi-autonomous flight capabilities, advanced sensors such as Light Detection and Ranging (LiDAR) and cameras, and robust safety mechanisms. The vehicle aims to enhance emergency medical transport, cargo delivery, and search and rescue operations, which demonstrates its feasibility and ease of deployment.

The remainder of this report is organized as follows. Section II presents the system overview of the proposed design. Section III provides an overall description of the developed vehicle comprising concept development, performance summary, and realized trade-offs. In Section IV, the multirotor configurations, propeller, and electric systems are discussed based on the battery characteristics. Section V focuses on justifying the major components and details of the autonomous system. Section VII, the communication, computational and obstacle detection modules are defined. Additionally, Section VIII discusses the competitive approach defined for each mission during the competition and the score calculation for each phase. Finally, Section IX provides the concluding remarks.

II. Systems Overview

This section outlines the system development approach, emphasizing the creation of the Concept of Operations (ConOps), shown in Figure 1, and the definition of top-level operational requirements that guided the development of the proposed vehicle.

A. ConOps

The competition operating system includes the Operating Crew (OC), who supervises the vehicle via the ground station, issuing directives and optionally controlling the vehicle manually. The ground station serves as the command and control center with real-time video and telemetry. The Competition Vehicle flies and completes missions, communicating with the Ground Station and interacting with the transport trailer and Payload Handlers (PH). Transportation comprises the transport vehicle and trailer for mission site arrivals. Payload handling involves human handlers and equipment like trolleys/stretchers for on-ground operations that interact directly with the vehicle in the Operating Zone (OZ). Objects of Interest are elements the vehicle approaches, such as unknown OZs or markers. Obstacles are elements to avoid, using an active Detect and Avoid System (DAS) for identifying and avoiding physical obstacles.

Simple missions like Mission 1, can be fully automated with pre-loaded flight profiles and onboard decision-making, while complex flights may require phases of high-level decisions by the OC at the Ground Station. A mission plan is a sequence of phases determined by the OC before takeoff. Phases may need user input during flight or be executed autonomously. The user can change the mission plan in real time by entering a “Mission Re-planning" phase. All phases included in the overall mission are Reconnaissance (Recon), Flight Operations (Hover, Cruise, Waypoint Visiting, Takeoff/Land), and Mission Re-planning.

The nominal operations for each mission are as follows. The initialization and setup for flight involves the OC configuring the ground station, mission plan, and vehicle. Preflight checks are automated where possible, including sensor calibration, power and propulsion verification, and ground station connections. Takeoff, flight, and landing operations are initiated by the OC, with the vehicle executing the mission plan and hovering when user input is required. The OC can

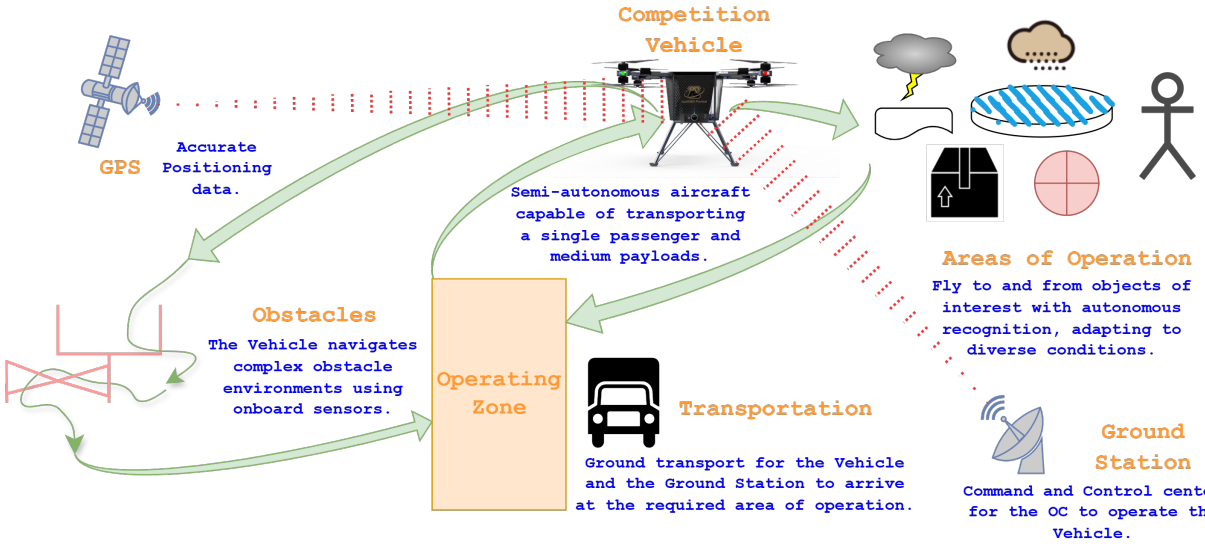

Figure 1: Concept of Operations Description

take manual control if needed.

Mission descriptions: Mission 1 (M1) involves one OC and active PH, with a fully automated flight plan and vehicle launch from the trailer. Mission 2 (M2) is semi-autonomous with under 30 seconds of OC input, involving no PH and one OC. The vehicle uses reconnaissance and flight phases, taking operator input to determine OZ and marker locations, then computing and executing the shortest path. Mission 3 (M3) is semi-autonomous with under 30 seconds of OZ input, involving active PH and one OC. The vehicle enters a Recon phase to detect obstacles and the OZ assigns “The Spot" via user input. Then the ground station computes the flight trajectory.

Packing and Storage/Transport: After a mission, the vehicle is moved back to the transport trailer within 10 minutes.

B. Requirements

To create a comprehensive set of operation requirements for the competition missions, a systematic approach was employed, integrating insights from various sources. The process began with a thorough analysis of the competition rules to ensure all mandatory criteria were met. This was followed by a detailed examination of the safety protocols, focusing on human factors to ensure safe operation. The development process was structured around the system and subsystem layers, ensuring that each component’s requirements were clearly defined and aligned with the overall mission objectives. By synthesizing information from these diverse sources, the team established a robust set of operational requirements, the top of which is depicted in Table 1.

III. Design Overview

The overall design started with a tradeoff analysis to define the energy source. Next, the concept generation and selection process was discussed, followed by a sizing overview specifying the system’s dimensions and capacities. The expected performance characteristics were then reviewed to highlight the system’s capabilities. To finalize the performance, analyses were accessed for each mission with detailed goals and expected outcomes for M1 (Productivity), M2 (Adversity), and M3 (Maneuvering).

Figures 2-5 show the current design from various perspectives to give a comprehensive visual understanding of the system. Figure 2 presents

Table 1: Operation Requirements

Label	Source	Requirement	Mission
OPER 2	1.2, 1.3	The vehicle must be capable of carrying a minimum payload of 57 kg.	M2, M3
OPER 5	2.2	The payload bay and flight operations are suitable for human usage.	M1, M2, M3
OPER 6	1.2	The aircraft dimensions fit within the minimum landing zone clearance.	M2
OPER 7	1.3, 2.5	The aircraft landing gear fits within the minimum landing zone clearance.	M3
OPER 9	2.3	The system must be able to be cleared within 10 minutes of mission completion.	M1, M2, M3
OPER 11	1.2	Land at an angle.	M1, M2
OPER 12	1.2	Land in harsh, non-uniform wind conditions.	M2
OPER 13	1.2	Withstand dusty environments.	M2
OPER 14	1.2	Withstand rain.	M2
OPER 18	1.3	Operate in GPS-denied environments.	M3
OPER 19	2.3	The vehicle must be safely and securely attached to its transport vehicle within the US highway legal limit and must be able to be quickly moved on ground.	M1, M2, M3

an isometric view, offering a three-dimensional perspective that highlights the overall structure and layout of the design. Figure 3 shows the front view, detailing the frontal dimensions and the arrangement of key components. Figure 4 provides a top-down view, depicting the layout and spatial distribution of the system's elements. Figure 5 displays the side view, which gives insight into the vertical profile and relative positioning of various parts.

Table 2 summarizes the design and system specifications, calculated using the sizing codes. The substantiation and justification of these specifications are provided in the subsequent subsections.

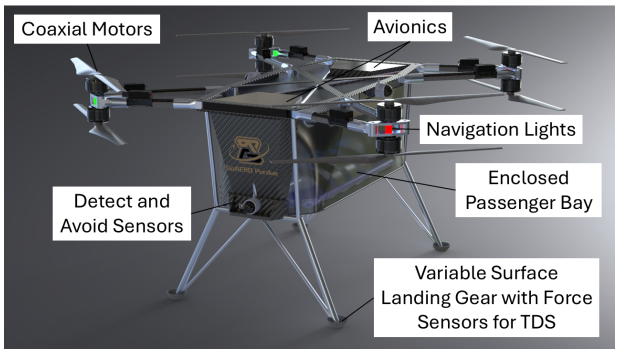

Figure 2: Isometric View of Designed Competition Vehicle

A. Energy Source Selection

A comprehensive trade-off analysis and technological assessment of innovative fuel options for the developed vehicle was conducted. The conclusions are summarized as follows:

Due to its high energy density, gasoline offers improved endurance. However, given our short flight times, this advantage is less significant. Additionally, installing distributed power plants is impractical due to mass and volume constraints. Achieving Vertical Take-Off and

Table 2: Design and System Specifications

Aircraft Parameters	**Values**
Flight time	20 min (Max load)
Cruise Speed	30 m/s
Empty Mass (Excl. Battery)	113 kg
Battery Mass	71 kg
Design Payload Capacity	87.6 kg
Max Payload Capacity	120 kg
Disk Loading	350 N/m^2
Power Loading	0.04 W/m^2
Dimensions incl. propellers	3.55 m * 3.76 m * 1.57 m
Propulsion System	
Number of Motors	8
Motor Configuration	Coaxial
Hovering Power	47.2 kW
Propeller Diameter	57 inches
Energy Source	Lithium-Ion Batteries

Figure 3: Front View of Designed Competition Vehicle

Figure 4: Top View of Designed Competition Vehicle

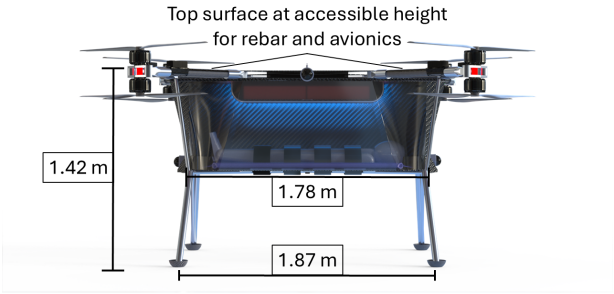

Figure 5: Side View of Designed Competition Vehicle

Landing (VTOL) would require either two rotors or complex mechanical transmissions to rotate multiple rotors with fewer engines.

The logistics of handling and developing fuel-powered systems, combined with safety concerns in the event of crashes, discouraged the team from using gasline as an energy source.

Hydrogen Fuel Cells (HFC) also have a higher energy density than batteries but lack sufficient power density. Our flight profiles involve limited cruising periods and extended power-heavy maneuvering, making HFCs an unsuitable option.

Battery solutions, on the other hand, offer high power density, are easy to transport, handle, and store, and do not significantly compromise performance given our flight profile. This is further validated by our baselines [1].

B. Concepts Generation and Selection

Using the morphological chart method, more than a dozen design concepts were generated. Table 3 describes the parameters used for the analysis.

Each aspect has multiple designs. By combining a design from each aspect, we generate a concept configuration for the vehicle. Varying the designs allows us to create new configuration ideas. All designs generated through this process were then evaluated using Pugh's method. Ultimately, four concepts were selected as the final design candidates, as shown in Figure 6.

Concepts 3 and 4 featured tilting rotors for thrust vectoring but were ruled out due to complexity and added weight. Preliminary weight

Table 3: Morphological Chart Overview

Aspect	Description
Payload	Payload storage designs for volume and placement
Lift	Design ideas for lift generation
Forwards Force	Design ideas for propelling the vehicle forward.
Landing	Design ideas for absorbing landing impact
Stability	Design ideas for maintaining stable flight in all conditions

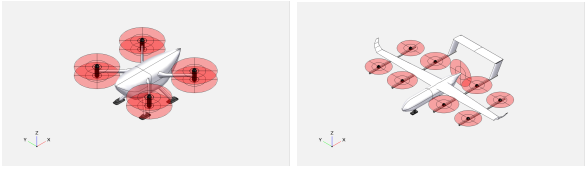

(a) Concept 1 (b) Concept 2

(c) Concept 3 (d) Concept 4

Figure 6: Concept Aircrafts

sizing was conducted to choose between Concepts 1 and 2. While Concept 2 was slightly lighter, its weight savings did not justify the loss in performance during maneuvering in Missions 2 and 3, which have very brief periods of cruise. The weight estimation methodology is presented in the next section.

C. Sizing Overview

Figure 7 illustrates the sizing process proposed. A multimode constraint analysis and two medium-fidelity energy-based sizing algorithms were developed to provide initial weight estimates for Concepts 1 and 2.

Figure 8 shows the constraint diagram, plotting the design space for a lift + cruise vehicle (Wing Loading) and a multi-rotor (Disk Loading) against their power loadings. The chosen design points are detailed in Table 2, which also includes the results from the iterative weight estimation code. Sizing was defined based on the flight profile of M1, as it requires the highest payload and flight time. A vehicle designed for M1 will also perform well in Missions 2 and 3, but the reverse may not be true. M1 offers multiple payload configurations. An optimization script was developed to find the configuration that maximizes the score in M1, defined as the aggregate payload mass over system mass. This score represents several complex trade-offs. Increasing the payload boosts the aggregate mass transported, but also increases the weight of the system. Heavier propulsion is needed to carry more weight, which in turn requires more batteries and a larger fuselage structure. In addition, a higher payload increases the workload during loading and unloading, which leads to more time spent on ground operations.

The time penalties for the ground operations at the optimal solution are given in Table 4. The algorithm incorporates the sizing code along with these time penalties to simulate scores in M1 for various payload masses. The payload

Table 4: Optimization Time Penalties

Parameter Name	Value (Metric)
Payload Load/Unload Time	2 min
Battery Swap Time	5.4 min
Alex Load Time	1 min

configuration that resulted in the highest score was chosen as the design point. The results are evaluated at different battery densities for robustness and are presented in Figure 9. Since many of the inputs (battery and payload swap times) are currently rough estimates, the vehicle is oversized to allow for flexibility. Although the optimal payload weight is 87.6 kg, comprised of 12 rebars and 3 sandbags. The vehicle is sized to carry a payload of 120 kg. A more robust strategy will be developed as better estimates for the swap times are established through testing and practice.

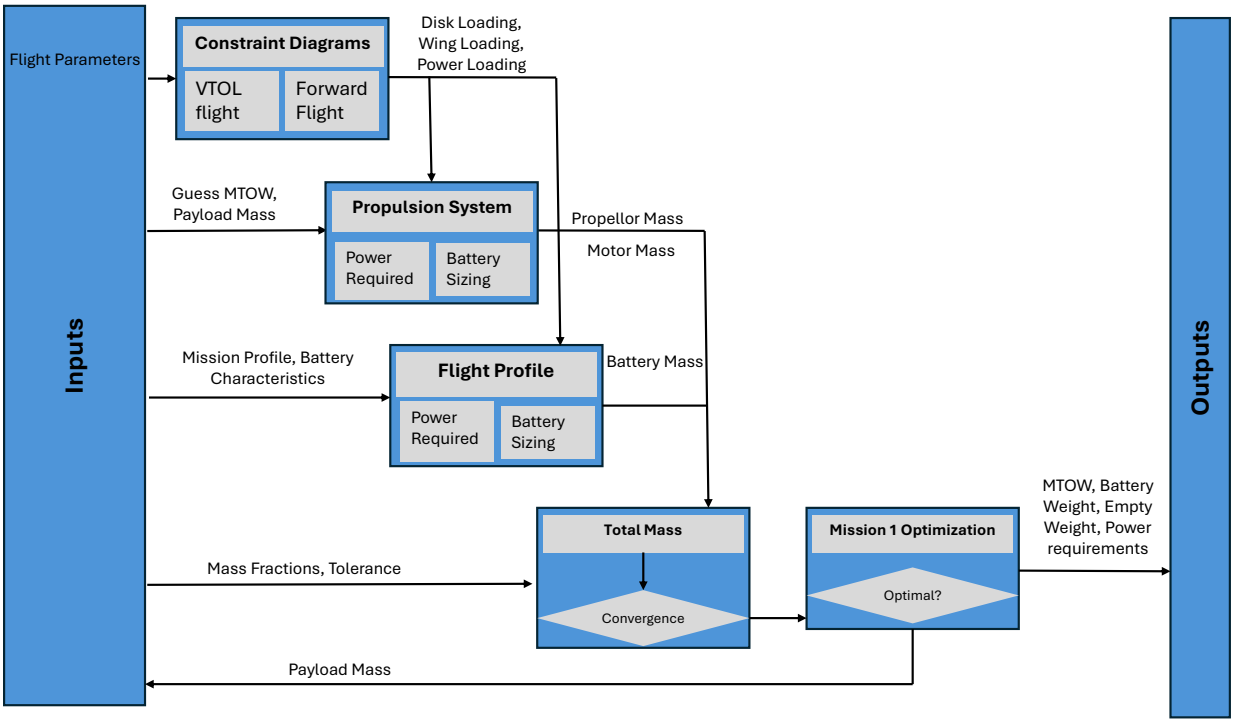

Figure 7: Sizing Methodology

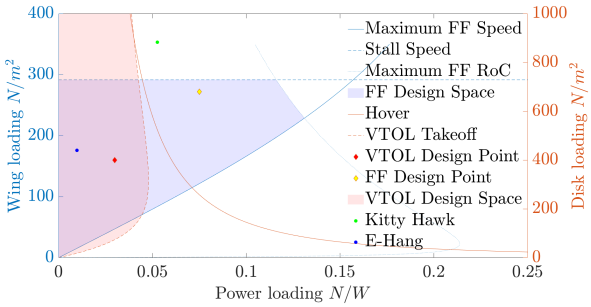

Figure 8: Multi Mode Constraint Diagram

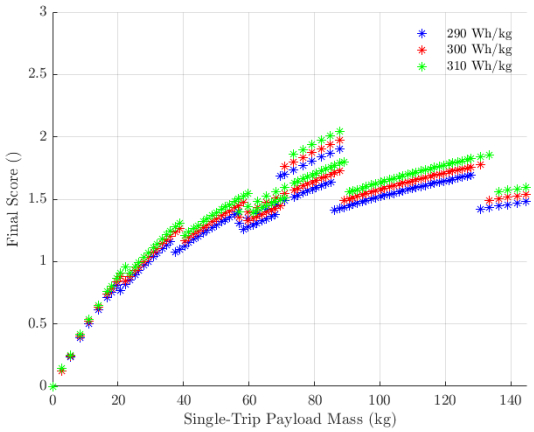

Figure 9: M1 Payload Optimization

D. Expected Performance Summary

The expected performance is summarized in in Table 2. An overview of each the system's performance in each mission is given below.

1. M1 (Productivity)

The expected flight time of each segment is approximately 2 minutes and 40 seconds, based on sizing results. The team iterated with various speeds to arrive at this value. Three battery swaps are planned, providing a flight endurance of 20 minutes plus a safety factor of 5 minutes for redundancy. The expected score is 2.28 with the optimized payload, with the total payload ferried being 1545 lb. .

2. M2 (Adversity)

Takeoff and landing performance has been estimated using prior art and power available, resulting in a takeoff velocity of 3 m/s and a landing velocity of 0.8 m/s.
Based on sizing results, takeoff time is 5 sec, flying over the marker and arriving to an OZ is 15 sec, mission OZ landing is 45 sec, flying back to the base is 10 sec and landing at the base is 20 sec. The ground pause is 120 sec and the Recon phase is 240 sec. This outputs a total time of 19 minutes and 55 seconds for M2.

3. M3 (Maneuvering)

The expected time of completion is 14 min and 50 sec. Based on sizing results, "The Base" takeoff time is 5 sec and landing time is 10 sec, "The Spot" takeoff time is 10 sec and landing time is 30 sec, Recon and Trajectory Planning phase is 3 min, obstacle course flight is 2 min 10 sec, and flight from "The Base" to the first obstacle is 20 sec. The takeoff and landing times in "The Spot" are longer than in "The Base", accounting for the extended time these may take due to "The Spot" being a GNSS denied zone.

E. Designed for Purpose Summary

This section summarizes the design features that enhance the competitive performance of the team. Table 5 highlights the principal sub-systems and their unique features. Each design element has been carefully considered in the context of the mission performance, efficiency, and usability.

F. Innovation and Enablers Summary

Table 6 summarizes unique subsystems, and descriptions of how these innovations enable the completion of the missions.

Table 5: Designed for Purpose Summary

Sub-system	**Feature**	**Description**
Payload Bay	Rapid loading	The payload bay access location enables rapid loading of Alex.
Payload Bay	External Net	Provides a modular for additional payload required in M1.
Airframe	Motor placement	The motors are high mounted to avoid obstructing the payload bay.
Landing Gear	Landing Gear Height	The landing gear is 0.7 meters long for the "Flood" OZ.

Table 6: Innovation and Enablers Summary

Sub-system	**Feature**	**Description**
Landing Gear	Hemispherical Gear Foot	Foot geometry inspired by aerospace applications designed to adjust for uneven terrains.
Power System	Plug-by-contact batteries	Employment of new technology to allow fast battery swaps.
Autonomy	Software	Path planning, Navigation, and DAS which reduce operator workload.

IV. Propeller Design and Power Systems Integration

A. Multirotor Configurations

From the Sizing Results, four motor configurations were considered: A quadrotor and a quad-octa with a co-axial setup, both in an X shape, a hexarotor, and an octa-rotor. A trade-off analysis was performed comparing the four different configurations. The disk area required to provide the thrust to perform all missions successfully, the power per motor required, access to the payload bay, and the compliance with the requirement stating that the propeller disk areas of must fit in a 15ft diameter circle (POW 3) were the factors considered in the comparison.

Table 7: Propulsion Requirements

Source	Label	Requirement	Mission
OPER 2, OPER 12	POW 1	Spacing between two center points of the disk areas in the direction of travel must be greater than 2.4 times the radius of the propellers.	M1, M2, M3
OPER 12	POW 2	Maximum input power must produce a thrust-to-weight ratio greater or equal to 2.	M1, M2, M3
OPER 6	POW 3	The propeller disk areas must fit in a circle of 15 ft in diameter.	M2
OPER 13, OPER 14	POW 4	The motor must be rated to at least IP-54 by the manufacturer.	M2

The distance between the center of gravity of the vehicle and the propulsion plane represents a tradeoff between stability and maneuverability. Placing the propulsion system higher up would decrease the effect of downwash, which is very relevant for the loose sand encountered in "The Pit" in M2. Furthermore, batteries are placed below the upper frame of the vehicle to minimize possible water damages in "The Flood" and allow easy access to Payload Handlers, shifting the center of mass towards the upper frame, incentivizing the motors to be placed towards the top of the vehicle.
However, this means the propellors may interfere with PH operations, as the propellor arcs overlap with the payload loading access points. A coaxial quadrotor represents the least amount of interference in this regard, followed by the quadrotor, the hex-copter, and finally, the octa-copter.

As a result of these analyses, the team selected the coaxial quad-rotor due to its ability to produce high thrust with an overall lower disk area in the xy plane, as well as for its minimal interference in payload handling. This allows the vehicle to comply with POW 3 while minimally interfering with access to the payload bay. Due to co-axial efficiency losses, greater electrical power must be provided to the motors than in the regular octa-rotor configuration, but the team concluded that these losses are not significant compared with having clear access to the payload bay and complying with POW 3.

B. Propeller Geometry and Spacing

The propeller's design is restricted by the motor selected and the complexities of designing a propeller. However, reducing the losses associated with wake interactions and interference between propellers is possible by managing spacing [2].

The induced velocity from vortex-vortex interactions decreases with the square of the distance from the core of the rotation area. These interactions must be delayed for as long as possible to allow these to space out from the plane of thrust, thus establishing requirement POW 4 [3].

Work in [4] finds that increasing the pitch of the lower propeller in a co-axial configuration outputs greater FM values, which conforms with Glauert's Theorem. According to the CFD testing [5] on the effect of vertical spacing, having a 0.1-0.15 H/D ratio is ideal. This is because the tip vortices from the upper propeller are preserved in the wake of the lower propeller and don't turn turbulent. A larger spacing of 0.5-1 H/D leads to increased upper propeller thrust but a drastically decreased lower propeller thrust because of a more turbulent wake and reduced overall performance. In order to account for the inefficiency mentioned in the sizing algorithm, the team assumed an inefficiency factor of 0.8 for each motor.

C. Battery Characteristics

A wide range of battery types for the vehicle were considered, but Lithium-Ion batteries were ultimately selected due to their high energy and mass density characteristics. Another benefit of these batteries is their overall availability in the market, which will eventually reduce the complexity and risk of the project by utilizing batteries that have been widely tested and safely approved for industry use.

To minimize vehicle mass and volume, our current estimates for battery energy density lie between 280 Wh/kg and 300 Wh/kg and a density between 2 kg/L and 2.5 kg/L, consistent with the advanced battery solutions available in the market. With the power parameters from the sizing results, POW 2, and test bench data from motor vendors, the maximum electrical power of each motor required is 16 kW, at the upper limit of payload of 120 kg as stated by the M1 optimization algorithm.

To visualize the variable power consumption of the motors in each stage of flight (as determined by sizing) and to validate POW 2 with a real-world motor, the electrical power required for each flight phase is provided in Fig 10. The power requirement is calculated using the empty and battery mass for a 120 kg payload, but assumes an 86.7 kg payload to allow flexibility for carrying additional mass in a single lap if strictly required to complete M1.

To make the electrical system redundant and reduce its localized total power, it will be split into two independent circuits, one for the top 4 motors and another for the bottom 4. Two battery modules of 18 L and 35.5 kg, with four battery packs in each module, are placed in the vehicle's battery compartment and power these two circuits separately. The battery size and weight are obtained through the sizing code by inputting the maximum payload of 120 kg.

Battery capacity will vary greatly depending on the possible voltage and amperage configurations. Our team has defined two alternatives listed below:

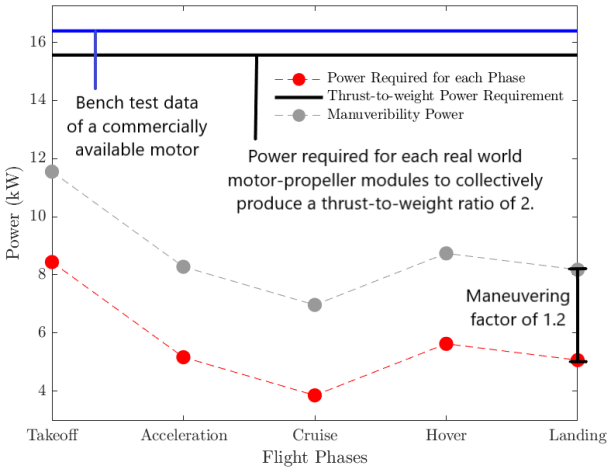

Figure 10: Electrical Power Required for Each Flight Phase

- 100V and 170A
- 400V and 42A

These voltages are the general upper and lower limits of the operating voltage of current electric motors that comply with our power requirements. Regardless of varying capacity, the batteries' discharge capacity (C) is constant. From mission performance estimates and sizing results, the maximum discharge rate required is 7C. This allows the Vehicle to produce an optimal thrust-to-weight ratio for safe maneuvering and rapid take-offs. The peak thrust-to-weight ratio is tentatively defined as a minimum of 2, as advised by technical research conducted on multirotor vehicles [6]. While this performance constraint governs maximum peak output thrust impracticable in standard operations, the required maneuvering and stabilization necessitate motors to produce this ratio so each motor can execute differential thrust.

Regarding battery sets, the team plans to perform battery swaps in order to sustain the great endurance required by M1, while maintaining a low battery mass for M2 and 3. By doing swaps in M1, the battery capacity will be sized around energy requirements for M2 and 3, making the Vehicle as light as possible. This imposes a time penalty on M1 due to the time taken when doing battery swaps, yet the benefits of reducing

weight far outweigh the time penalty the team will face. Avionics has a separate battery that is not swapped.

D. Electric System Characteristics

The high electrical power required to fly the vehicle requires an analysis regarding PH safety when swapping batteries and the heat management of the system. The main trade-off lies in the voltage and amperage selected for the electronics. A high voltage and low current may avoid the necessity of liquid battery cooling and increase the system's efficiency. Still, this would pose a risk to the PH, who will be manually handling this high-voltage system.

If the electronics are designed to support lower voltages and more significant current, liquid battery cooling will likely be required to prevent battery failure or the risk of spontaneous combustion, as observed in electric vehicles of a comparative scale. Introducing liquid cooling to the system would significantly increase its complexity and weight. Thus the team identifies extrema of the motor voltage (100V and 400V) and current range. A system with 250V and 68A, serving as an example, would likely require both liquid cooling and extended safety measures, which introduces two types of disadvantages to the system.

To avoid the increased mass, power draw, and complexity of including liquid battery cooling in the system, increasing the output voltage of the batteries and selecting a motor compatible with the system's voltage would be optimal.
However, we recognize the safety concerns raised by PH's manual handling and hot-swapping 400V batteries. To aid with the battery hot-swap timing and minimize PH's interaction with the system's electric terminals, the batteries will be slid in and connected to a plug-by-contact port. This means that PH will never have to touch the terminal to connect the battery to the vehicle, reducing the risks mentioned and the time taken in battery swaps.

V. Design Justification

A. Airframe

The airframe must fit within a 15-foot diameter space in its flight-ready state to guarantee a landing in "the unknown" OZ in M2. In addition, the airframe must meet the transport dimension restrictions. Other design criteria include placement of the motors, and adequately transferring loads of landing and lifting for the entire system. All these requirements are presented in Table 8. The front and top views of the airframes are shown in Figs. 3 and 4, respectively.

The upper frame configuration achieves the dimension requirements by placing the rotors such that the propeller tips are at the edge of the 15 ft diameter, maximizing the front-to-back separation of the rotors and the allocated fuselage space. This separation also creates 2.31 meters of unobstructed space on the side of the airframe, allowing Alex to be loaded from the side. To mount the coaxial motors, the frame must secure them to ensure stable flight characteristics, minimize turbulence, and provide adequate airflow near the cooling intakes and ample spacing for wiring and mounting access. Each motor is mounted on its own aluminum plate, including openings for its bottom cooling intakes. These plates have ample spacing in between them to provide the cooling airflow and access to the mount screws and wiring. Between these motor mount plates, two aluminum couplers act as spacers, connecting the motor mounts to the arms of the frame. Sorbothane padding will be used at this connection to dampen vibrations generated by the motors from the rest of the airframe. Sorbothane isolation in unstable quadcopter results in a 15 percent reduction in the mean difference between maximum and minimum noise [7]. With a loss factor of 0.2-0.3, Sorbothane allows a greater proportion of vibrations to be converted and released from the system as heat in comparison to other common material choices like rubber. The attachment point will use Betaforce composite

Table 8: Upper Frame Requirement

Source	Label	Requirement	Mission
M1, M2, M3	UF 1	The upper frame must satisfy all geometry requirements for motor positioning.	M1, M2, M3
OPER 5	UF 2	Dampens vibration of propulsion system.	M1, M2, M3
OPER 19	UF 3	The width of the vehicle is less than the US legal highway limit of 8.5' with additional contingency (minimum 0.5') on either side.	M3

bonding adhesive. It has a low shear modulus, further contributing to the reduction in vibrations being passed to the airframe.

Two cylindrical arms hold each coaxial set for structural redundancy, shown in Figure 11. This provides mounting surfaces for the two Electronic Speed Controllers (ESC) required for each coaxial set and ensures that the motor axes are vertically oriented. The ESCs are oriented upward, facing the downwash of the top propeller for effective cooling. The wiring will be run along each arm with covers to protect against environmental factors.

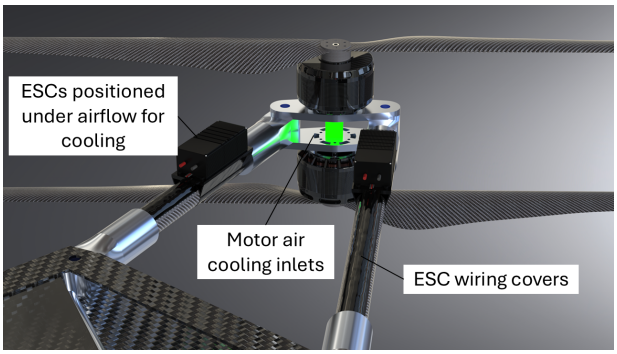

Figure 11: Arm and Motor Mounts

There are multiple objectives for the lower section of the frame, including connecting the landing gear and payload bay to the upper frame, ensuring spacing on the sides of the fuselage for accessing payload and batteries, and providing an adequate load path from the landing gear to the upper frame. During flight and landing, loads will be distributed to the upper frame. The lower frame transfers load upwards and contains the airframe features relevant to mission scoring. To effectively integrate with the upper frame, the lower frame connects to the arm couplers and contains spars between the upper frame panels. This frame also supports the battery compartment to ensure the heavy mass of the batteries is supported. The upper frame will also store the avionics in the front and rear sections, where there is access to the sensor and ESC wiring. This location also isolates the components from the heat generated by the battery, which is held by the center of the upper frame. To be lifted for transport, the lower frame contains spars at the bottom of the fuselage, providing a strong surface from which the airframe can be lifted. Sorbothane will again be used here as a method of mitigating landing impulse. It outperforms other common load dampeners like rubber and neoprene, as it diminishes the force within a similar time frame with a lower maximum force experienced [8].

To simplify our assembly process, the multirotor extension arms comprise round carbon-fiber tubes, a proven industrial solution for multicopters that may be sourced from external manufacturers. A roll-wrapped plain weave tubing is currently preferred due to its superior torsional load and crush resistance. Still, a pultruded construction provides greater unidirectional load resistance and stiffness. Further structural analysis may reveal additional compelling reasons to use pultruded construction.

B. Payload Bay

The primary roles of the payload bay are to provide effective payload storage, ease of loading, and adequate passenger environment. Table. 9 outlines requirements governing our design of the payload bay.

Both side loading and back loading config-

Table 9: Payload Bay Requirement

Source	Label	Requirement	Mission
OPER 11-18	PB 1	The payload bay must provide mounting points for and satisfy all geometry requirements to position sensors and electronics components.	M1, M2, M3
OPER 2, OPER 5	PB 2	The payload bay must house "Alex" securely and comfortably.	M2, M3
OPER 2	PB 3	The payload bay must house all additional payloads required for the productivity mission.	M1
OPER 2, 5, 9	PB 4	The payload bay must provide clear access to payload handlers.	M1, M2, M3

urations were considered for the payload bay. Comparison of numerous concepts resulted in the selection of a side loading design as shown in Figure 12. This eliminates the need for a sliding system for the stretcher, supplies easy access to all areas of the bay, and proves to be ultimately lighter for all configurations. Since battery swaps will happen alongside loading or unloading Alex, the battery bay is also accessed through the payload bay as this creates a more efficient loading process. The Vehicle's center of gravity must be placed near the motors as this increases the aircraft's maneuverability for M3. Placing the batteries near the bottom of the bay facilitates battery loading, but significantly reduces maneuverability. It also introduces additional heat dissipation challenges, as this heat moves toward the passenger. There is also an increased risk of water entering the battery bay at "The Flood" OZ. Considering all this, the battery bay is located at the top of the payload bay.

The payload bay must secure Alex to minimize flight instability and maximize passenger safety. This system must be effective, lightweight, and quick to operate within the allocated payload loading time. Using adjustable straps proved to be much lighter and simpler than alternative securing mechanisms while remaining efficient for the payload handlers.

As the extra payload (sandbags and rebar) is only utilized in mission one, the most optimized

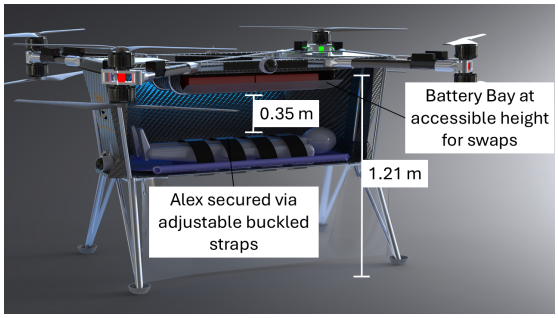

Figure 12: Isometric View of Payload Bay Internals

design involves an external system to contain this payload that can be removed for the remaining missions where it is unnecessary. However, this system must fulfill the requirements of secure storage while being lightweight and efficient to load. In comparing multiple configurations and mounting hardware options, the most efficient and lightweight option is to have a removable net under the fuselage to ferry the sandbags in mission one. A cargo net from US Cargo Control with E-track mounting hardware was chosen, as this fitting system is optimized and designed to take extremely high loads while remaining highly modular and easy to remove/attach. These mounting plates are very light and can be left attached for the remaining missions without a detriment to performance. The net also includes cam buckles, which allows it to be properly tightened in order to effectively secure the extra payload in place during flight. The rebars can be secured to the top of the frame, where they are at an accessible

height of 1.42 meters.

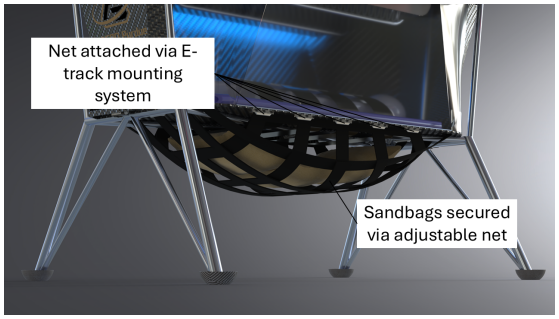

Figure 13: Sandbag Storage

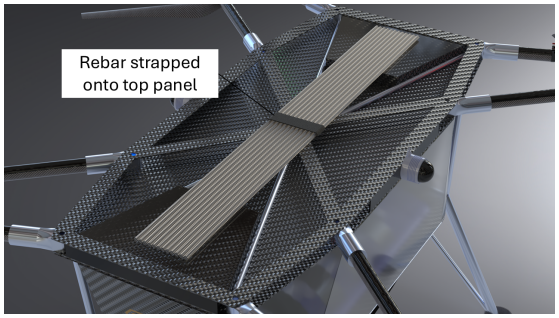

Figure 14: Rebar Storage

Similarly, considering the necessity to maintain a lightweight structure to enhance general flight performance and, more critically, allow for an ideal center of mass position, carbon fiber composites have been identified as a primary material candidate for payload mechanisms due to their inherent strength-to-mass ratio. A geometrically simple structural design composed of predominantly flat panels allows large-scale carbon prepreg laminates to be utilized. This is advantageous compared to typical wet-layup or resin infusion manufacturing processes due to their superior tensile strength and stiffness. It also allows for using honeycomb core sandwich panels to improve the strength-to-mass ratio further, allowing for significant weight reduction.

C. Landing Gear

This section discusses the trade-offs in landing gear design. The landing gear's requirements are summarized in Table 10.

While the team intends to hover over the water's surface for "the flood" OZ, the gear must still elevate the payload bay over the water line as an added redundancy. This results in a trade-off where longer landing gears make the system prone to tipping and add weight. The landing gear must also comply with the minimum landing zone and transportation restrictions. According to these requirements, a hemispherical shape is used at contact points with the ground to maintain effective contact with uneven surfaces, shown in Figure 16. This design performs well in unstable environments and has been used for lunar landers.

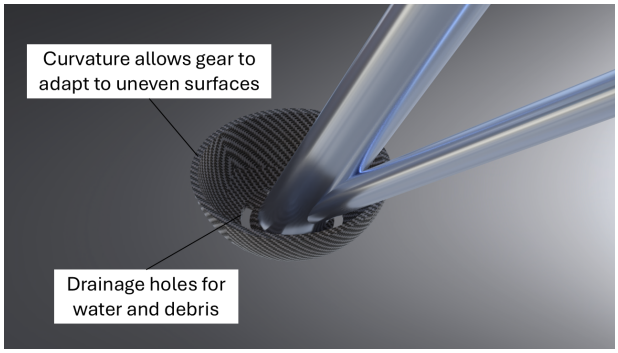

Figure 15: Landing Gear Foot

A touchdown detection system is incorporated through the use of a force transducer at the foot of the gear. This allows for accurate landing detection, improving safety and mission speed. The legs attach to the frame under the bay, distributing landing forces throughout the airframe. Sorbothane will be implemented within the frame and to dampen vibrations and impulses during landing. Due to the advantages of carbon fiber composites discussed previously,and simple molding procedures, it was chosen as the material for the landing gear feet. There are significant challenges with using metal/plastic for such structures.

VI. Autonomy System Specifications and Justification

In executing the previously discussed mission strategies, The system must be capable of securing all the Autonomy points for M1 and partial

Table 10: Landing Gear Requirement

Source	Label	Requirement	Mission
M1, M2, M3	LG 1	The landing gear must accommodate the TDS.	M1, M2, M3
OPER 5	LG 2	Dampens impact and does not intrude fuselage.	M1, M2, M3
OPER 6, 7	LG 3	Does not exceed 8ft landing zone diameter.	M1, M2, M3
OPER 11	LG 4	Gear makes flush contact with rugged terrain.	M2
OPER 13, 14	LG 5	Gear elevates fuselage and is resistant to environmental wear.	M1, M2, M3
OPER 19	LG 6	Must be easily and effectively transported.	M1, M2, M3

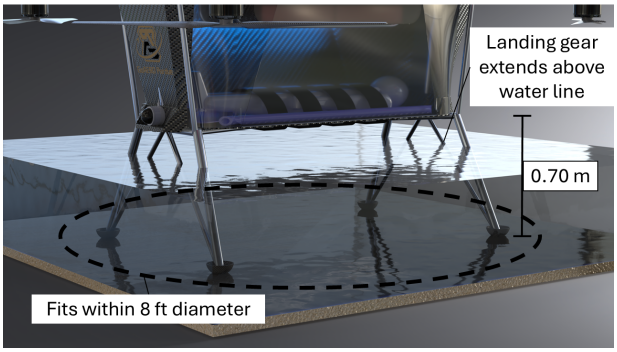

Figure 16: Landing Gear

autonomy points for Missions 2 and 3. The overall Autonomy architecture is first discussed, followed by a description of the flow of information through the autonomy stack for each mission.

The overall architecture is comprised of the following essential components:

• Autopilot: The autopilot system includes the hardware that consists of sensors to be used in all missions: global positioning system (GPS), Altimeters, and inertial measurement units (IMUs), and the software responsible for sensor fusion/state estimation to provide the high-level computer and the ground station an accurate estimate of the system state at all times. The autopilot system will also be directly responsible for following the trajectory/Way-points generated by the ground station via low-level control of the motors to achieve the desired state.

• High-level computer: Our high-level computer is an embedded system that will handle all decision-making and autonomy-related computations that will be performed onboard. It will be responsible for communications between the vehicle and the ground station/OC for all missions. In addition, it will handle (along with the ground station/OC) all contingency operations in the case of critical system failure (loss of communications, GPS malfunction, loss of propulsion systems). It will monitor the critical systems status using information from the autopilot and power/electronics system. It also hosts the flight plan manager that stores the trajectory/way-points generated by the ground station. The computer will also be responsible for executing the following programs:

– Detect-and-Avoid: The high-level computer, using LiDAR information is able to identify obstacles along the flight path.

– Flight Planning: Upon identifying obstacles along the flight path, a path planning algorithm based on the optimized rapidly exploring random tree method [9] will be applied to generate obstacle avoidance paths in real-time.

– Simultaneous Localization and Mapping (SLAM) Navigation: In the event of GPS loss, the computer will safely navigate the vehicle using LiDAR SLAM method, with the known positions of objects of interest (markers, operating zones, objects) assisting in navigation.

– Touchdown Detection System: The computer should be able to detect when the vehicle lands and keep the vehicle on the ground for a desired time duration.

• Ground Station: The ground station will be responsible for relaying information from the OC to the vehicle. These include signals to begin or terminate missions, or to allow the OC to override the existing flight plan. It will also be responsible for high-level computations that include pattern recognition and trajectory/way-point generation

using our path planning algorithms, and then transmitting this information to the high-level computer for execution.

• Electrical System: The electrical system consists of the batteries, which provide power to the motors and other peripherals onboard the vehicle (sensors, high-level computer), the ESCs used for motor-control, and the motors.

In addition to this, the various phases of operation are also described below:

• General Flight Profile Phase: These contain the following commands with their inputs, including take off, hover, cruise, land, and navigate to waypoints.

• Recon: To convert visual camera-fed data to GPS coordinates for waypoints, which uses computer vision algorithms.

• Mission Re-planning: During this phase, the OC may make changes to the flight plan while the vehicle hovers or cruises.

The OC arranges a flight plan before takeoff. A flight plan is defined as a sequence of general or recon phases. During the flight, the vehicle may enter an Editing Phase, which pauses all operations and allows the OC to make changes to the flight plan or flight parameters. A generic information flow diagram can be found in Figure 17.

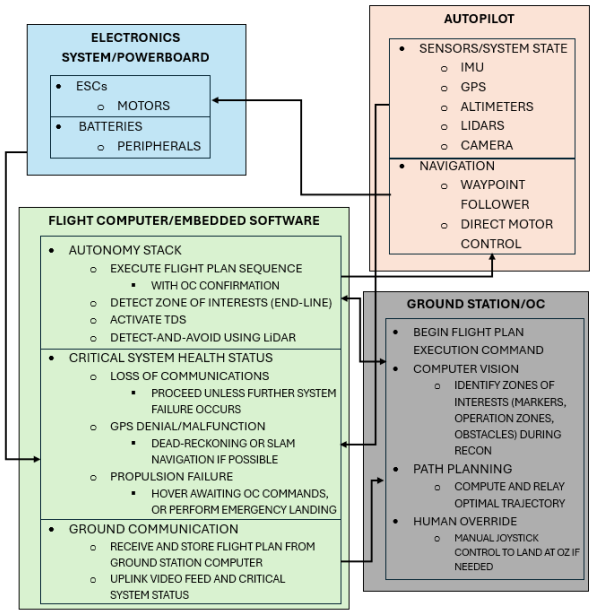

Figure 17: Information Flow diagram of Autonomy system

VII. Avionics and Sensors Specifications and Justification

The vehicle's avionics systems comprise all the electronics onboard, excluding the propulsion system (Batteries for motors). The aviation system includes the communication module, the computation module, the obstacle detection module, and the general sensing module.

A. Communication Module

The current concept of operations requires various information to be presented to the OC to enable their high-level decision-making. This information comprises:

• Video feeds from various angles (primarily forwards and downwards)

• GPS location and vehicle pose

• State of battery

• Time of flight

• Current mission phase and the next mission phase.

• Objects of interest, e,g., obstacles, targets, landing zones

This is ordered according to the priority level in the event of a weak signal/reduced bandwidth. Higher priority items will be transmitted first. Due to the high data rate demands of transmission, the UHF (Ultra-High Frequency)radio set has been selected as the candidate for managing communications due to the high data transfer rate, a high frequency radio will be used. 5.6 Ghz radio data links are commonly used in live video transmission in drones, and is a strong candidate for our communications.

B. Computation Module

The computation module comprises the autopilot, the high-level computer, and the ground station module. Subject to further evaluation, the team will source components to satisfy these roles. While determining the split between ground-

based computations and onboard computations, the primary considerations are:

• Computation Speed: Ground-based computers can be more powerful, reducing computation time. However, communication latencies must be accounted for.

• Safety: In the event of loss of communication to the ground. The Onboard system must have the capabilities to safely handle the situation independently.

In compliance with these considerations, it was determined that all Recon activities and analysis would be completed on the ground station. The vehicle will receive a planned trajectory post recon from the ground station, and the onboard computer can track it with an active Detect and Avoid program via onboard LiDARs. However, trajectory generation will be done at the ground station. Pattern recognition and vision/contour processing will also be used. The onboard computer will store the planned mission/paths and compute system health status, low-level commands for the motors, and decision-making such as the DAS.

C. Obstacle Detection Module

The LiDAR placement used for mapping and obstacle detection is shown in Figure 18. The field-of-view (FOV) of the LiDAR is 360° horizontally and 90° vertically, detecting points in a right-angled cone with a range of 30 meters. The coverage is not complete; however, it is satisfactory for detecting the obstacle locations for M3.

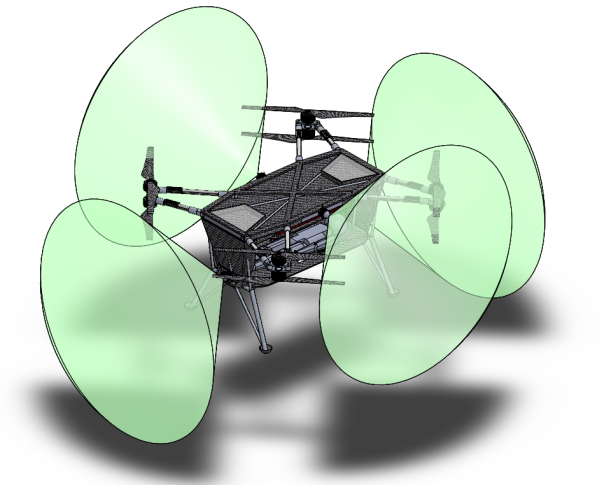

Figure 18: Detect and Avoid Sensor Coverage

VIII. Competitive Strategy

This section discusses the competitive strategy to be executed for the three missions. An overview of the targeted points and worst-case scenarios for score estimations is provided.

A. Mission 1

To decrease empty weight in M1 the robust sensor and communication packages required for M3 will be removed. The team intends to launch directly from the transport trailer in less than 5 minutes and finish the mission fully autonomously without any user input. To facilitate an autonomous landing, the vehicle's landing zone is set via the GPS coordinates of the truck plus some offset to represent the OZ. To aid this, the truck will be parked on the trapezoidal OZ's longer side or base. The team will transition the vehicle and the trailer from a transport-ready to a flight-ready state within 5 minutes. The ground station will be set up during the touch-free timer pause of 20 minutes. To aid this rapid set up and deployment, the team intends to use 2 OCs for this mission.

The vehicle will attempt to autonomously sense the end line via its vision-based sensors to determine the turning point. The vehicle only detects results within a region close to the approximate 0.25-mile mark to avoid false detection. The vehicle finishes the segment flight profile as such and then autonomously lands. Status lights are used to indicate that the vehicle is safe to approach.

B. Mission 2

M2 aims to complete landings in OZ with various conditions in the shortest time. Performing automated landings in diverse and actively changing conditions of different operation zones is a

competitive design feature that the team aims to achieve. Considering the penalties of landing outside the OZs, the OC will observe the vehicle's position before landing and correct it manually if needed. By positioning the vehicle inside the OZ, the vehicle lands autonomously inside the OZ boundaries with the goal of minimizing operator input while ensuring no mission penalties for the team. Only one OC will be used for this mission to earn the 2-point bonus.

The team designed a unique flight profile to make semi-autonomous operations possible. After takeoff, the vehicle enters the Recon Phase to identify the location of each OZ and the marker. The vehicle will then start flying between the marker and OZs. Upon arrival, the vehicle hovers above each OZ, detects its type using cameras and, if necessary, user input, and performs a pre-programmed procedure for landing in that condition. Since the team has the option to hover over the OZ, while the landing gear is in contact with the OZ, the team chooses to do this for "The Flood" zone. For The Hill, The Pit, and The Tornado, the vehicle will perform a standard landing procedure. The vehicle enters another Recon Phase for "the unknown" zone while hovering over the OZ. During this phase, the OC indicates, via camera feeds on the interface, all obstacles to the system, and the system then determines the optimal landing zone and executes it.

The system utilizes the touchdown detection system to detect and time a landing. This touchdown detection system combines the vehicle's altitude and force readings from the landing gear to detect a landing. This reduces the workload of the OC since now they do not have to time the system's landing. This also enables the system to initiate an automated takeoff exactly when the 2-minute requirement for a landing is met to avoid any human-related latencies.

C. Mission 3

In the Maneuvering Mission, our strategy focuses on rapid and precise obstacle navigation, using LiDAR based obstacle avoidance and visual camera recognition. The vehicle configuration for M3 includes the robust sensor and communication packages described in Section VII.

The OC in this mission employs one person to target the bonus points. During the first lap, the vehicle enters a Recon Phase, detecting obstacles and "The Spot" with OC inputs. Using pattern recognition, the vehicle can then assign obstacle identities to each pylon. The vehicle now plans a trajectory using these obstacle locations in compliance with the mission instructions.

The vehicle now tracks this trajectory with the Detect and Avoid system active. This system uses LiDAR readings to avoid collision with an obstacle in real-time. For all operations in "The Spot", the vehicle will rely on dead reckoning and inputs from the OC. The OC may intervene here if necessary.

D. Points Overview

Based on the strategy designed for each mission, the team expects to earn 91 competition points without considering the ranking points, as shown in Table 11.

Table 11: Points Strategy

Mission	1	2	3	Total
Competition	25	25	25	75
Bonus Points				
Operating Crew	0	2	2	4
Workload	4	2	2	8
Deployment	4	NA	NA	4

IX. Concluding Remarks

This report described the development of a semi-autonomous aerial transport vehicle for the GoAERO competition. Designed for emergency and critical environments, the vehicle is powered by lithium-ion batteries. Key design choices include a coaxial quadrotor configuration to optimize thrust and payload handling. The autonomy

system, supported by advanced avionics and sensors, ensures efficient navigation and obstacle avoidance.

The competitive strategy emphasizes rapid deployment, autonomous operation, and precise obstacle navigation to maximize performance. The vehicle's design and systems integration aims to enhance emergency medical transport, cargo delivery, and search and rescue operations while also being tailored specifically for the competition.

References

[1] Magnino, A., Marocco, P., Saarikoski, A., Ihonen, J., Rautanen, M., and Gandiglio, M., "Total cost of ownership analysis for hydrogen and battery powertrains: A comparative study in Finnish heavy-duty transport," *Journal of Energy Storage*, Vol. 99, 2024, p. 113215.

[2] Shukla, D., and Komerath, N., "Multirotor Drone Aerodynamic Interaction Investigation," *Drones*, Vol. 2, No. 4, 2018. https://doi.org/10.3390/drones2040043, URL https://www.mdpi.com/2504-446X/2/4/43.

[3] Dougherty, S., Oo, N. L., and Zhao, D., "Effects of propeller separation and onset flow condition on the performance of quadcopter propellers," *Aerospace Science and Technology*, Vol. 145, 2024, p. 108837.

[4] Kim, Y. T., Park, C., and Kim, H. Y., "Three-Dimensional CFD Investigation of Performance and Interference Effect of Coaxial Propellers," *2019 IEEE 10th International Conference on Mechanical and Aerospace Engineering (ICMAE)*, 2019, pp. 376–383. URL https://api.semanticscholar.org/CorpusID:204861961.

[5] Yoon, S., Lee, H. C., and Pulliam, T. H., "Computational study of flow interactions in coaxial rotors," *AHS Technical Meeting on Aeromechanics Design for Vertical Lift*, 2016.

[6] Goli, S., Kurtuluş, D. F., Alhems, L. M., Memon, A. M., and Imran, I. H., "Experimental study on efficient propulsion system for multicopter UAV design applications," *Results in Engineering*, Vol. 20, 2023, p. 101555.

[7] Miller, D. S., *Open loop system identification of a micro quadrotor helicopter from closed loop data*, University of Maryland, College Park, 2011.

[8] Alrashdan, A., Alsumait, A., and Es-Said, O., "Material selection of an elastomer capable of absorbing vibrations actuated by a 4d movie theater," *Journal of Failure Analysis and Prevention*, Vol. 17, 2017, pp. 376–384.

[9] Noreen, I., Khan, A., and Habib, Z., "Optimal path planning using RRT* based approaches: a survey and future directions," *International Journal of Advanced Computer Science and Applications*, Vol. 7, No. 11, 2016.